MARGINAL FERMI LIQUID IN TWISTED BILAYER GRAPHENE

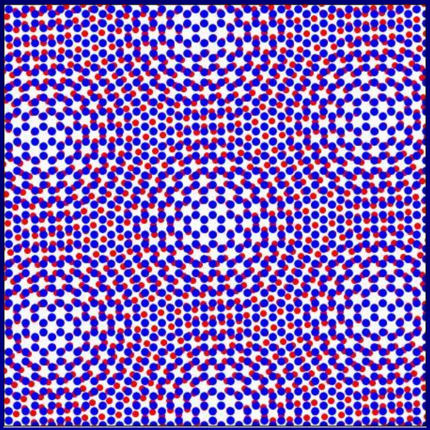

J. González[1] and T. Stauber[2]

[1]Instituto de Estructura de la Materia, CSIC, Spain

[2]Instituto de Ciencia de Materiales de Madrid, CSIC, Spain

TWISTED BILAYER GRAPHENE

Magic-angle twisted bilayer graphene is a system with a very reach phase diagram, showing strong correlations and superconductivity about half-filling of the moiré superlattice

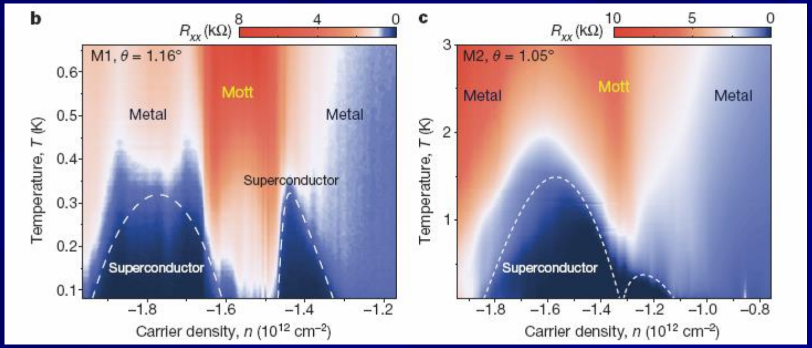

Y. Cao, V. Fatemi, S. Fang, K. Watanabe, T. Taniguchi, E. Kaxiras, and P. Jarillo-Herrero, Nature 556, 43 (2018)

Similar observations have been carried out at other filling levels of the first valence and conduction bands

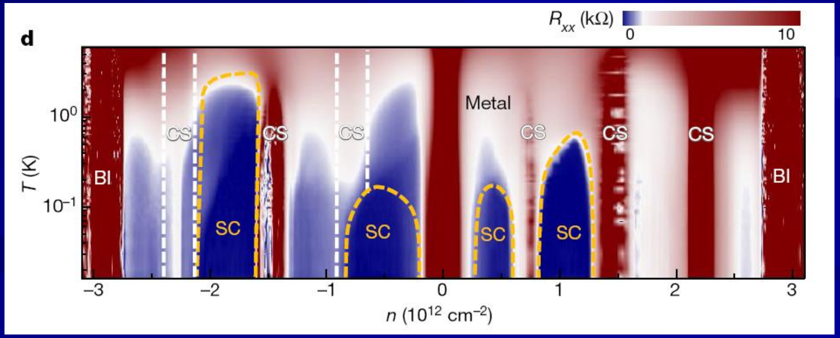

X. Lu *et al.*, Nature 574, 653 (2019)

TWISTED BILAYER GRAPHENE

Near half-filling, *T*-linear resistivity is observed above the superconducting dome

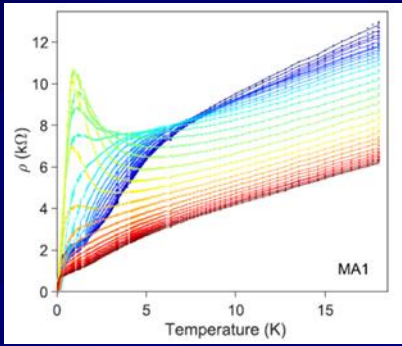

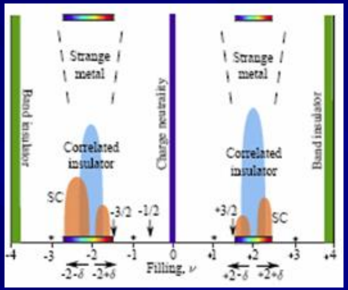

Y. Cao, D. Chowdhury, D. Rodan-Legrain, O. Rubies-Bigordà,
K. Watanabe, T. Taniguchi, T. Senthil, and P. Jarillo-Herrero,
Phys. Rev. Lett. 124, 076801 (2020)

These measurements give important information about the electron quasiparticles, which reflect in turn the low-energy dispersion and Fermi lines of the electron system.

TWISTED BILAYER GRAPHENE

We have to bear in mind that the low-energy bands are never completely flat in twisted bilayer graphene, and that relevant topological features arise as the magic angle is approached. This can be shown with the continuum model, where the coupling between the two layers can be varied smoothly

single valley picture

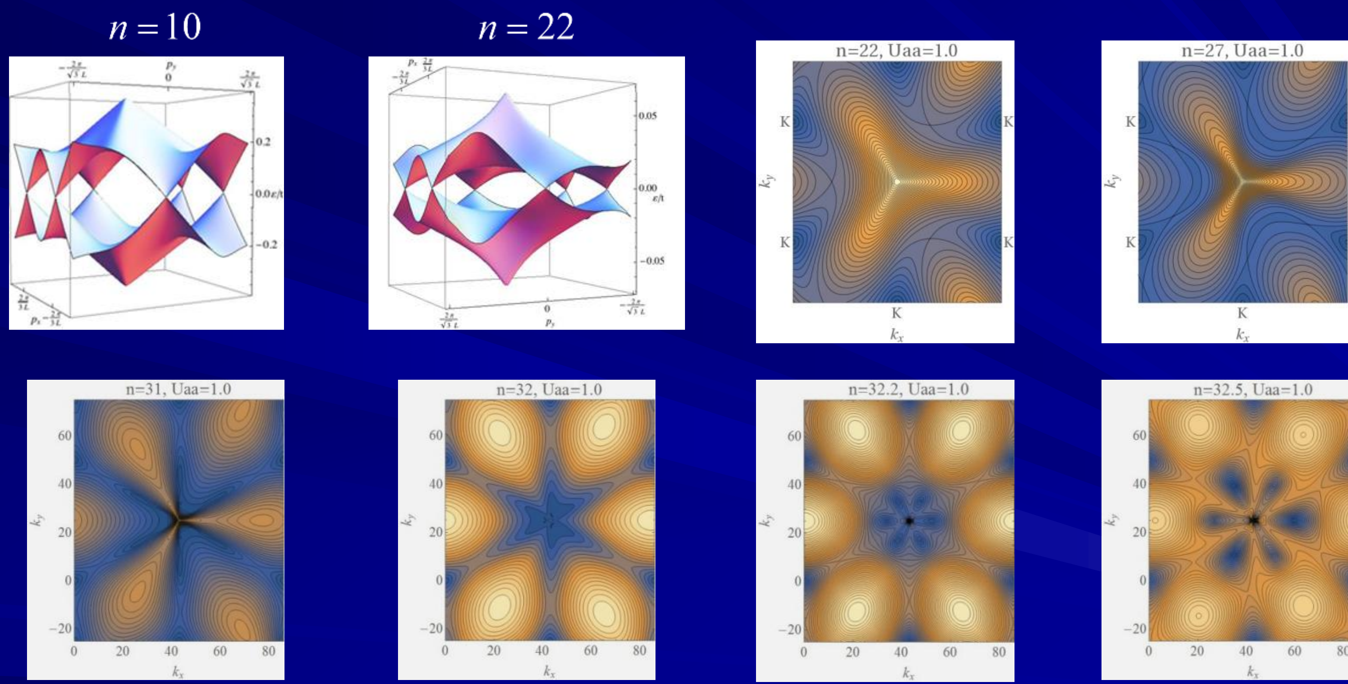

The bands are never flat, but there is a critical value of the interlayer coupling strength at which the symmetry is enlarged from C_{3v} to C_{6v} , which causes the effective compression of the bandwidth of valence and conduction bands.

TWISTED BILAYER GRAPHENE

The complete picture is obtained by superposing the low-energy bands from the two graphene valleys at K and $-K$

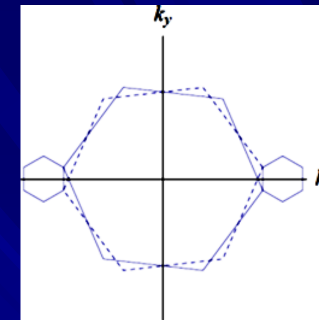

$$E_{\mathbf{k}}^{+} = \max\left(E_{\mathbf{k}}^{K}, E_{\mathbf{k}}^{-K}\right) \quad , \quad E_{\mathbf{k}}^{-} = \min\left(E_{\mathbf{k}}^{K}, E_{\mathbf{k}}^{-K}\right)$$

1st valence band E^{+}

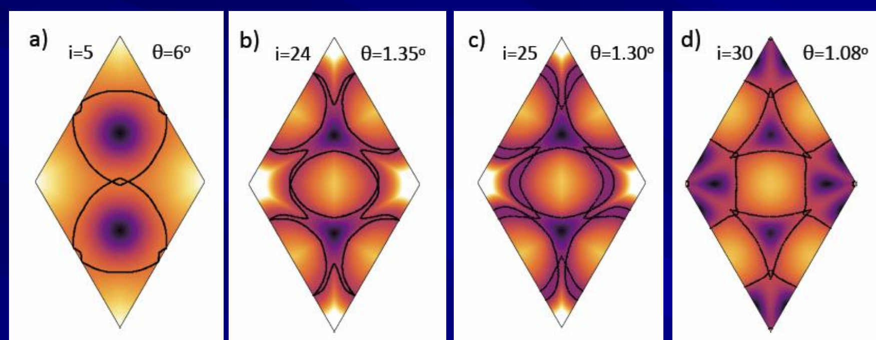

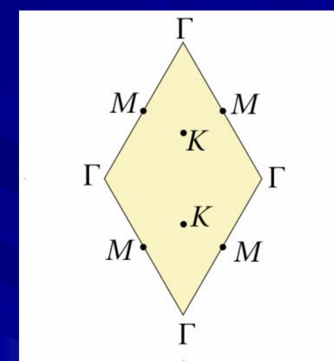

2nd valence band E^{-}

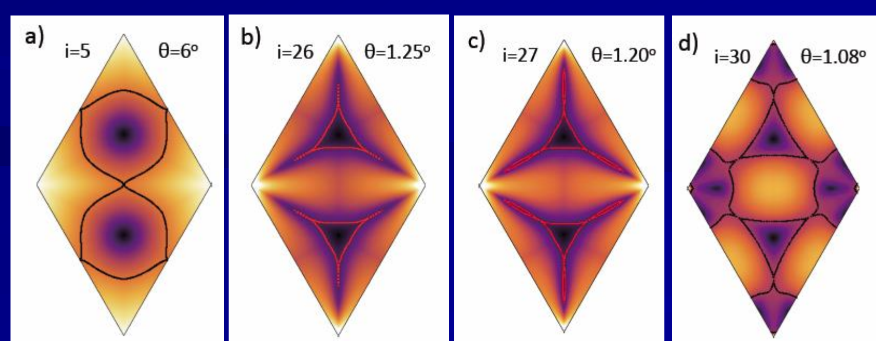

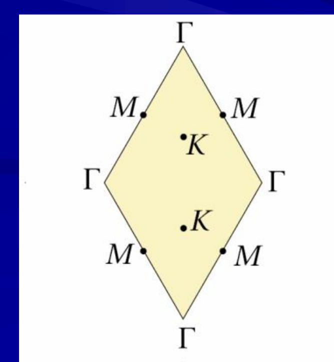

TWISTED BILAYER GRAPHENE

A more accurate method to compute the low-energy bands in the twisted bilayers is the tight-binding approach. The hamiltonian can be written in terms of various hopping matrix elements within and between layers 1 and 2

$$H = -\sum_{\langle i,j\rangle} t_{\|}(\boldsymbol{r}_i - \boldsymbol{r}_j)\,(a^{\dagger}_{1,i}a_{1,j} + h.c.) - \sum_{\langle i,j\rangle} t_{\|}(\boldsymbol{r}_i - \boldsymbol{r}_j)\,(a^{\dagger}_{2,i}a_{2,j} + h.c.) - \sum_{(i,j)} t_{\perp}(\boldsymbol{r}_i - \boldsymbol{r}_j)\,(a^{\dagger}_{1,i}a_{2,j} + h.c.)\,.$$

A common parametrization is

$$-t(\mathbf{d}) = V_{pp\pi}(d)\left[1 - \left(\frac{\mathbf{d}\cdot\mathbf{e}_z}{d}\right)^2\right] + V_{pp\sigma}(d)\left(\frac{\mathbf{d}\cdot\mathbf{e}_z}{d}\right)^2$$

$$V_{pp\pi}(d) = V^0_{pp\pi}\exp\left(-\frac{d-a_0}{r_0}\right)\;,V_{pp\sigma}(d) = V^0_{pp\sigma}\exp\left(-\frac{d-d_0}{r_0}\right)$$

The tight-binding model gives a reliable picture of the low-energy bands when approaching the magic angle

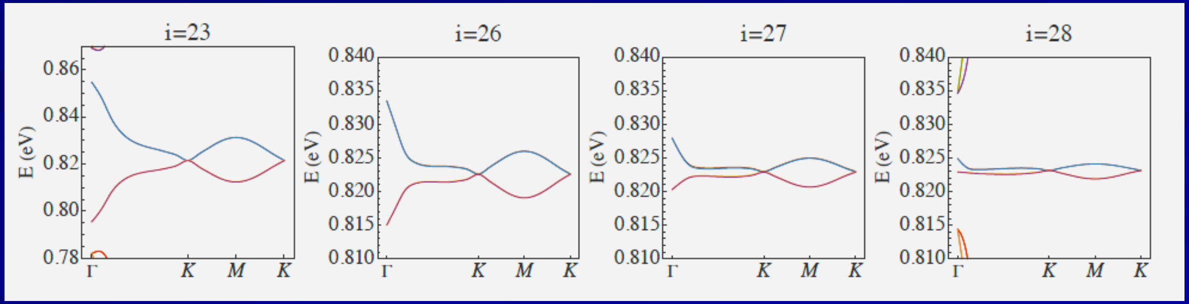

TWISTED BILAYER GRAPHENE

The evolution of the saddle points in the continuum model compares very well with that in the tight-binding approach

continuum model
1st valence band

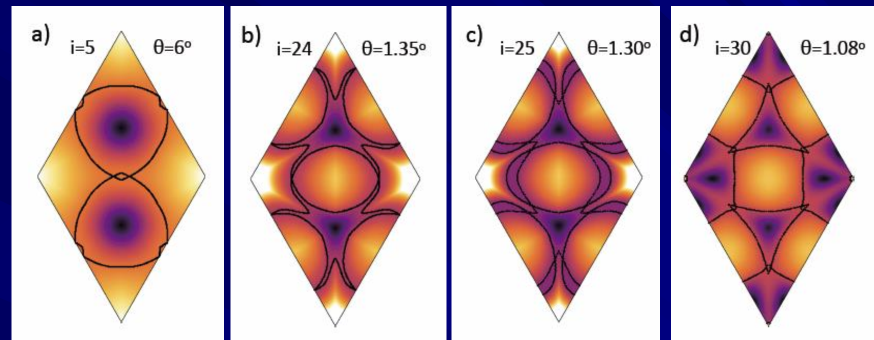

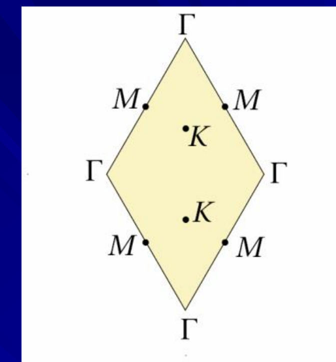

tight-binding model
1st valence band

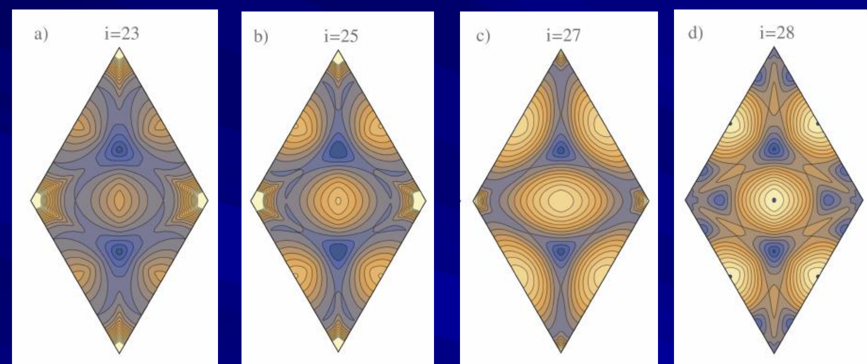

But the tight-binding approach allows to resolve the hybridization along the ΓK line

tight-binding model
2nd valence band

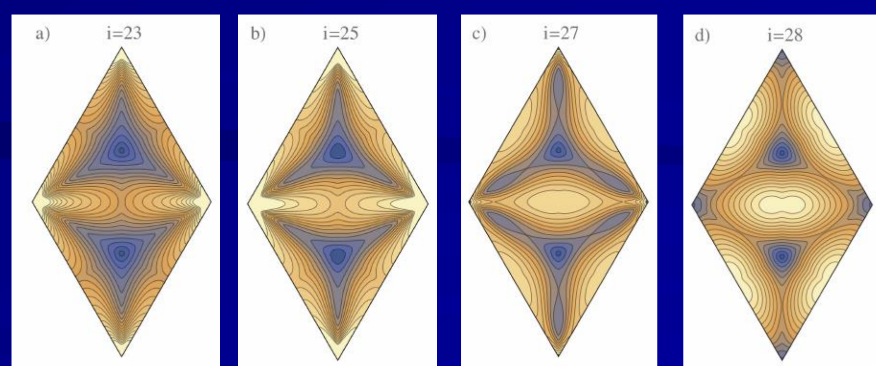

J. G. and T. Stauber,
PRL **122**, 026801 (2019)

MARGINAL FERMI LIQUID IN TWISTED BILAYER GRAPHENE

Near half-filling, *T*-linear resistivity is observed above the superconducting dome

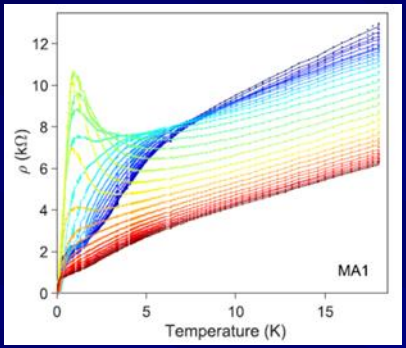

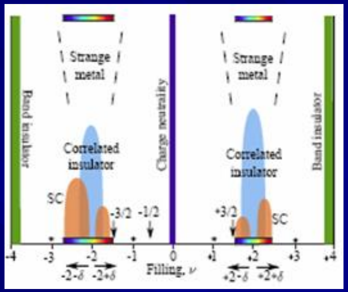

Y. Cao, D. Chowdhury, D. Rodan-Legrain, O. Rubies-Bigordà,
K. Watanabe, T. Taniguchi, T. Senthil, and P. Jarillo-Herrero,
Phys. Rev. Lett. 124, 076801 (2020)

This is a very challenging observation since electron-phonon scattering cannot account for such an effect at temperatures $T \sim 1$ K

$$\rho_{e-ph} \propto T^5 \quad , \quad T << \Theta_D$$

MARGINAL FERMI LIQUID IN TWISTED BILAYER GRAPHENE

We can turn to the effects of *e-e* scattering, which are rather strong given the extended character of the saddle points at the ΓK line

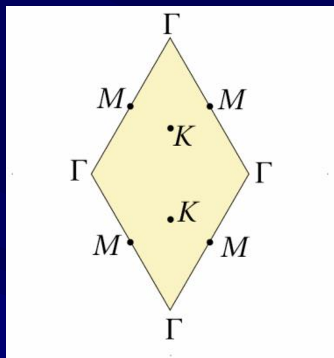

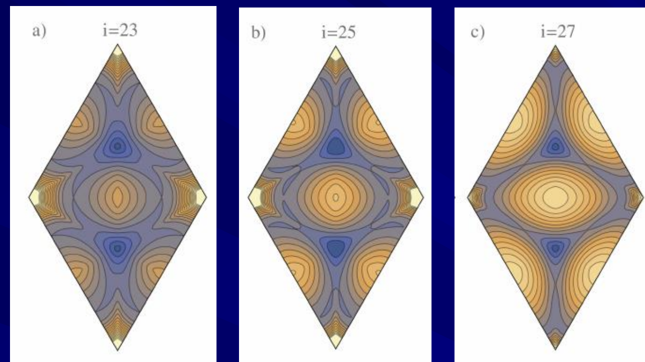

$\Longrightarrow$

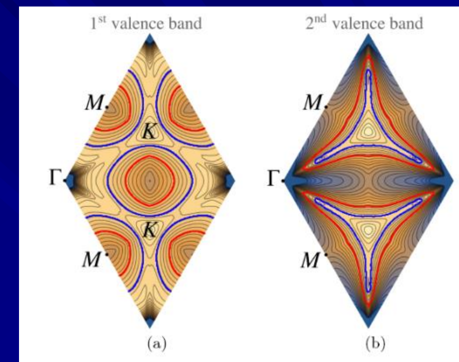

MARGINAL FERMI LIQUID IN TWISTED BILAYER GRAPHENE

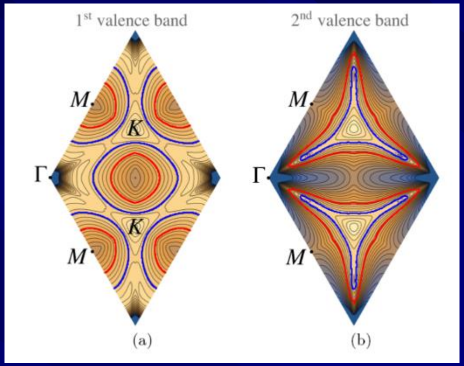

Near the magic angle, the straight segments of the Fermi line around the saddle points of the 2nd valence band give rise to a large peak in the electron-hole susceptibility

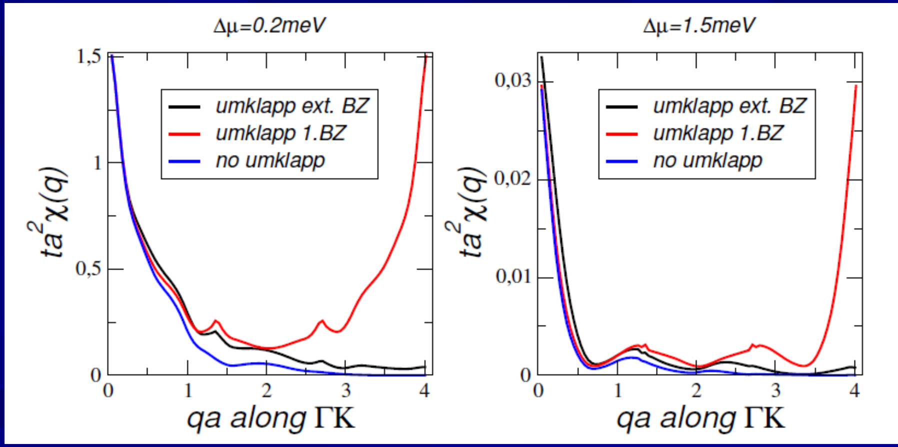

MARGINAL FERMI LIQUID IN TWISTED BILAYER GRAPHENE

The enhanced susceptibility has an important impact on the transport decay rate

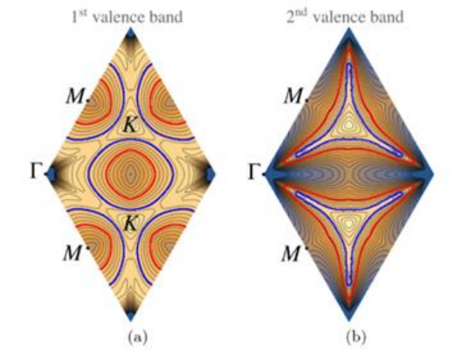

$$\frac{1}{\tau_{\rm tr}^{(ij)}(\boldsymbol{k})} = U^2 \int \frac{d^2k'}{(2\pi)^2} \int_0^{\varepsilon_{\boldsymbol{k}}^{(i)}} d\omega \, |\langle i,\boldsymbol{k}|j,\boldsymbol{k}'\rangle|^2 \times (1-n_F(\varepsilon_{\boldsymbol{k}'}^{(j)}))\,\delta(\varepsilon_{\boldsymbol{k}}^{(i)}-\varepsilon_{\boldsymbol{k}'}^{(j)}-\omega)\,{\rm Im}\chi_{\rm tr}^{(ij)}(\boldsymbol{k},\boldsymbol{k}';\omega)$$

$${\rm Im}\chi_{\rm tr}^{(ij)}(\boldsymbol{k},\boldsymbol{k}';\omega) = \int \frac{d^2p}{(2\pi)^2}|\langle l,\mathbf{p}|l',\mathbf{p}+\boldsymbol{k}-\boldsymbol{k}'\rangle|^2 n_F(\varepsilon_{\mathbf{p}}^{(l)})(1-n_F(\varepsilon_{\mathbf{p}+\boldsymbol{k}-\boldsymbol{k}'}^{(l')})) \left[(\boldsymbol{v}_{\boldsymbol{k}}^{(i)}+\boldsymbol{v}_{\mathbf{p}}^{(l)}-\boldsymbol{v}_{\boldsymbol{k}'}^{(j)}-\boldsymbol{v}_{\mathbf{p}+\boldsymbol{k}-\boldsymbol{k}'}^{(l')})\cdot\boldsymbol{n}\right]^2 \delta(\varepsilon_{\mathbf{p}+\boldsymbol{k}-\boldsymbol{k}'}^{(l')}-\varepsilon_{\mathbf{p}}^{(l)}-\omega) \quad (1)$$

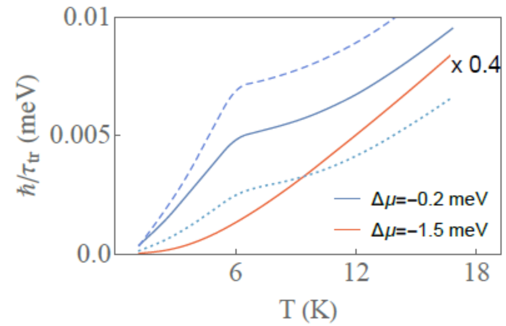

FIG. 2. Plot of the temperature dependence of the values averaged over the Fermi line (and weighted with the inverse of the square of the Fermi velocity to get dimensions of energy) of $1/\tau_{\rm tr}^{(11)}$ (dashed line), $1/\tau_{\rm tr}^{(22)}$ (solid line) and $1/\tau_{\rm tr}^{(12)}$ (dotted line), when the Fermi level is 0.2 meV (blue curves) and 1.5 meV (orange curve, scaled by a factor of 0.4) below the vHS.

J. G. and T. Stauber,
PRL **124**, 186801 (2020)

MARGINAL FERMI LIQUID IN TWISTED BILAYER GRAPHENE

The resistivity has a direct dependence on the transport decay rate

$$\rho_{\boldsymbol{n}} = \rho_0 \frac{\frac{1}{T}\int \frac{d^2k}{(2\pi)^2}\frac{n_F(\varepsilon_{\boldsymbol{k}})}{\tau_{\rm tr}(\boldsymbol{k})}}{\left(\int \frac{d^2k}{(2\pi)^2}\frac{\partial n_F(\varepsilon_{\boldsymbol{k}})}{\partial \varepsilon_{\boldsymbol{k}}}(\boldsymbol{v_k}\cdot \boldsymbol{n})^2\right)^2}$$

In our two-band model, we can discern between separate contributions

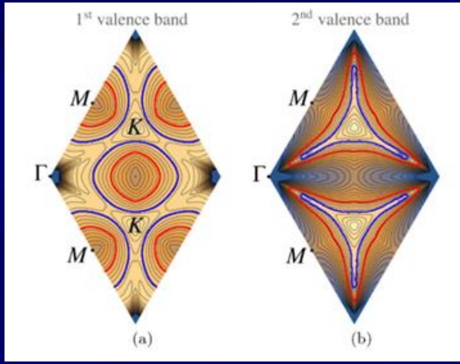

$$\rho_{ij} \sim \rho_0 \frac{1}{T}\oint_{\mathcal{C}_i} dk_\parallel \int \frac{d\varepsilon^{(i)}_{\boldsymbol{k}}}{v^{(i)}_{\boldsymbol{k}}}\frac{n_F(\varepsilon^{(i)}_{\boldsymbol{k}})}{\tau^{(ij)}_{\rm tr}(\boldsymbol{k})}$$

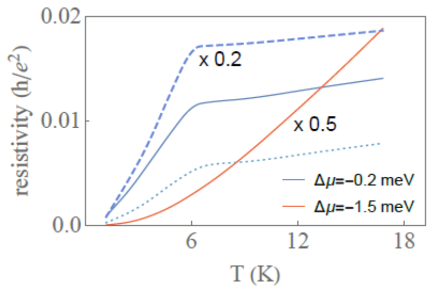

FIG. 3. Plot of the temperature dependence of ρ_{11} (dashed line, scaled by a factor of 0.2), ρ_{22} (solid line) and ρ_{12} (dotted line), for a shift of the Fermi level $\Delta\mu = -0.2$ meV (blue curves) and -1.5 meV (orange curve, scaled by a factor of 0.5) with respect to the level of the vHS.

J. G. and T. Stauber, PRL **124**, 186801 (2020)

MARGINAL FERMI LIQUID IN TWISTED BILAYER GRAPHENE

Not only the resistivity, but also quasiparticle properties display unconventional behavior

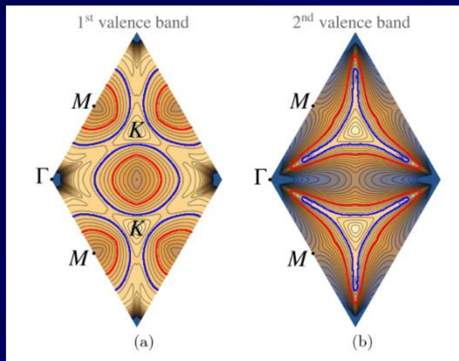

$$\mathrm{Im}\,\Sigma^{(ij)}(\boldsymbol{k},\omega) = -U^2 \int \frac{d^2p}{(2\pi)^2} \int_{-\infty}^{\infty} d\omega_p \, |\langle i,\boldsymbol{k}|j,\mathbf{p}\rangle|^2$$
$$\times \,\mathrm{sgn}(\omega_p)\,\delta(\omega_p - \varepsilon_{\mathbf{p}}^{(j)})\,\mathrm{Im}\,\chi(\boldsymbol{k}-\mathbf{p},\omega-\omega_p)$$

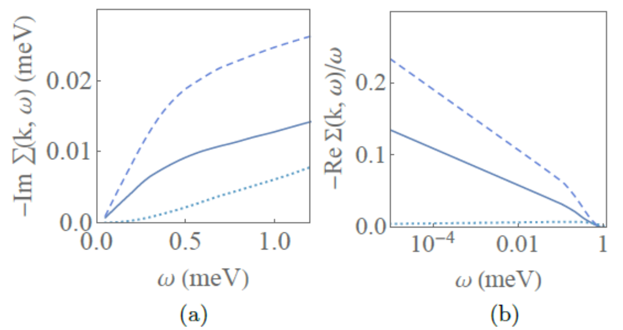

FIG. 4. Plot of the frequency dependence of the real and the imaginary part of the values averaged over the Fermi line of $\Sigma^{(11)}$ (dashed line), $\Sigma^{(22)}$ (solid line) and $\Sigma^{(12)}$ (dotted line), for a shift of the Fermi level $\Delta\mu = -0.2$ meV below the vHS.

The anomalous scaling of the electron self-energy characterizes the so-called marginal Fermi liquid behavior, with a progressive attenuation of the quasiparticles when approaching the Fermi level

$$G(\mathbf{k},\omega) = \frac{1}{\omega - \varepsilon_{\mathbf{k}} - \Sigma(\mathbf{k},\omega)} \sim \frac{1/|\log(\omega)|}{\omega - \varepsilon_{\mathbf{k}} + i\gamma\,\omega}$$

J. G. and T. Stauber,
PRL **124**, 186801 (2020)

MARGINAL FERMI LIQUID IN TWISTED BILAYER GRAPHENE

$$G(\mathbf{k},\omega) = \frac{1}{\omega - \varepsilon_{\mathbf{k}} - \Sigma(\mathbf{k},\omega)} \sim \frac{1/\left|\log(\omega)\right|}{\omega - \varepsilon_{\mathbf{k}} + i\gamma\,\omega}$$

The marginal Fermi liquid behavior is also reflected in quantities like the entropy of the electron liquid

$$S \sim \frac{1}{T}\int \frac{dk_{\|}}{v_{\mathbf{k}}}\int_{-\infty}^{\infty} d\omega\,\omega\,\frac{\partial n_F(\omega)}{\partial\omega}\left(\omega - \mathrm{Re}\,\Sigma(\mathbf{k},\omega)\right)$$
$$\sim T\left|\log(T)\right|$$

We end up with the prediction that a number of observables should be affected by the anomalous scaling

heat capacity $\quad C = T\frac{\partial}{\partial T}S \sim T\left|\log(T)\right|$

thermal conductivity $\quad \kappa(T) = \alpha\, C \sim \left|\log(T)\right|$

MARGINAL FERMI LIQUID IN TWISTED BILAYER GRAPHENE

A second important consequence of the transport measurements is that they imply very large values of the transport decay rate (Planckian scattering)

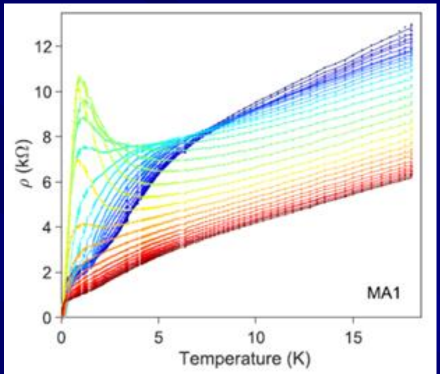

Y. Cao *et al.*, Phys. Rev. Lett. **124**, 076801 (2020)

Our model cannot account for Planckian scattering with just a Hubbard interaction, but we can reach the Planckian regime by computing with the long-range Coulomb interaction in the RPA

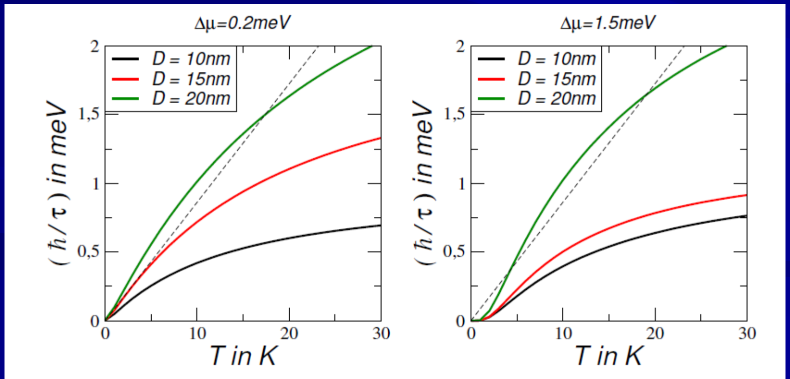

FIG. 5. The scattering rate $\hbar/\tau$ of TBG with $i = 29$ as function of the temperature for two chemical potentials around the vHS and screened long-ranged interaction with surrounding dielectric material $\epsilon = 5$. D denotes the distance of TBG to the top and bottom gate. The dashed line indicates the Planckian scattering rate $\hbar/\tau = 0.086 meV \cdot T[K]$.

J. G. and T. Stauber, PRL **124**, 186801 (2020)

TWISTED BILAYER GRAPHENE

In conclusion,

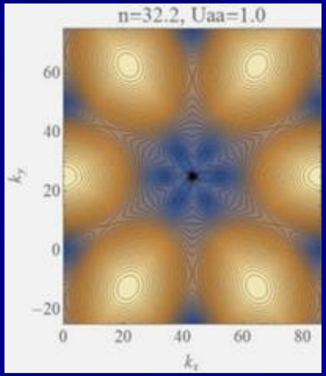

- The low-energy bands of twisted bilayer graphene show a remarkable evolution, which seems to be rather universal as the ΓK lines act as an attractor of the saddle points in the first valence and conduction bands when the magic angle is approached

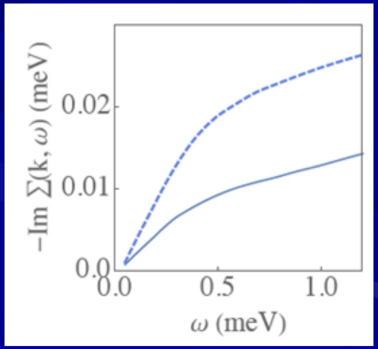

- Experimental signatures like the *T*-linear behavior of the resistivity above the superconducting dome can be explained in the framework of a model with enhanced *e-e* interaction around the saddle points. However, the magnitude of the resistivity seen in the experiments is too large to be reached in weak coupling approaches to the transport decay rate